Defect Structure in Thin Films of a Lamellar Block Copolymer Self-Assembled on Neutral Homogeneous and Chemically Nanopatterned Surfaces

Sang Ouk Kim,* Bong Hoon Kim, and Kwanghyon Kim

Department of Materials Science and Engineering, Korea Advanced Instituted of Science and Technology(KAIST), Daejeon, Republic of Korea 305-701

Chong Min Koo

LG Chemicals, 104-1, Moonji-dong, Yuseong-gu, Daejeon, Republic of Korea 305-380

Mark P. Stoykovich and Paul F. Nealey

Department of Chemical & Biological Engineering and Center for Nanotechnology, University of Wisconsin, Madison, Wisconsin 53706

Harun H. Solak

Laboratory for Micro- and Nanotechnology, Paul Scherrer Institute, CH-5232 Villigen PSI, Switzerland

Received January 13, 2006; Revised Manuscript Received May 11, 2006

ABSTRACT: Various defect structures in a symmetric block copolymer self-assembled in thin films on neutral homogeneous and chemically nanopatterned surfaces were investigated. On neutral homogeneous surfaces, a lamellar morphology lacking long-range order was observed with a high density of defects such as dislocations and disclinations in the two-dimensional plane of the film. On chemically patterned surfaces, the commensurability between the periodicity of the surface pattern and the block copolymer lamellae determined the final structure. When the surface pattern period was commensurate with the natural lamellar period, well-registered defect-free lamellar structures were obtained. In contrast, if the length scales were incommensurate, the formation of new structures such as dislocation dipoles, undulated lamellae, and tilted lamellae was observed. Our present work provides a detailed analysis of these new defect structures. In particular, a model describing the three-dimensional structure of the undulated morphology is suggested.

Introduction

Self-assembled nanostructures of block copolymer thin films have gathered significant attention due to their potential application as lithographic templates for the fabrication of photonic band-gap materials,[1] ultrahigh-density nanodots[2,3] or nanowire arrays,[4,5] memory and capacitor devices,[6] and nano-patterned substrates for biosensors. Despite their advantages such as parallel processing, molecular level resolution, and the capability to generate three-dimensional structures, the practical application of block copolymer thin films has been limited. The lack of a robust strategy to control the structure formation in thin film geometries has been considered a major obstacle. Various methods such as graphoepitaxy,[7,8] chemical surface treatments,[9,10] the application of external fields,[11−13] directional solidification,[14,15] and solvent aging[16,17] have been developed to control the orientation of the block copolymer nanodomains.

Epitaxial self-assembly using chemically nanopatterned surfaces has been demonstrated to be a successful strategy for controlling the orientation and long-range ordering of block copolymer nanostructures in thin films. Chemically nanopatterned surfaces have been prepared and used to perfectly register the self-assembled nanostructures of the block copolymers, thereby providing well-defined nanopatterns over arbitrarily large areas.[18,19] In this approach the commensurability between

the surface pattern period and the lamellar period has been found to play a crucial role in determining the final structure. When the pattern periods are incommensurate, various defect structures appear. However, a detailed analysis of the defects has not yet been undertaken. Here we report on the analysis of defects that arise in thin films of diblock copolymers that are self-assembled on neutral homogeneous and chemically nanopatterned surfaces. The investigation of these defects provides the first step toward understanding the relationship between the interfacial energy at the film−substrate interface and the nanostructure evolution.

The chemically patterned surfaces were prepared by selective oxidation of the self-assembled monolayer (SAM) surface using advanced lithographic techniques. The obtained pattern consisted of alternating neutral and polar SAMs. The pattern period (stripe width of neutral SAM plus stripe width of polar SAM) ranged from 45 to 55 nm. A symmetric block copolymer having an equilibrium lamellar period of 48 nm was self-assembled on those surfaces. The details of the block copolymer morphology were investigated with a particular emphasis on the defect structures.

Experimental Section

A symmetric poly(styrene-*block*-methyl methacylate) copolymer (PS-*b*-PMMA) was purchased from Polymer Source, Inc. and used without any further purification. The molecular weight of block copolymer was 104 kg/mol (PS block: 50 kg/mol; PMMA block: 54 kg/mol). The lamellar period of the spontaneously formed structure was determined from a SEM image of disordered lamellae.

* To whom correspondence should be addressed: e-mail sangouk.kim@kaist.ac.kr.
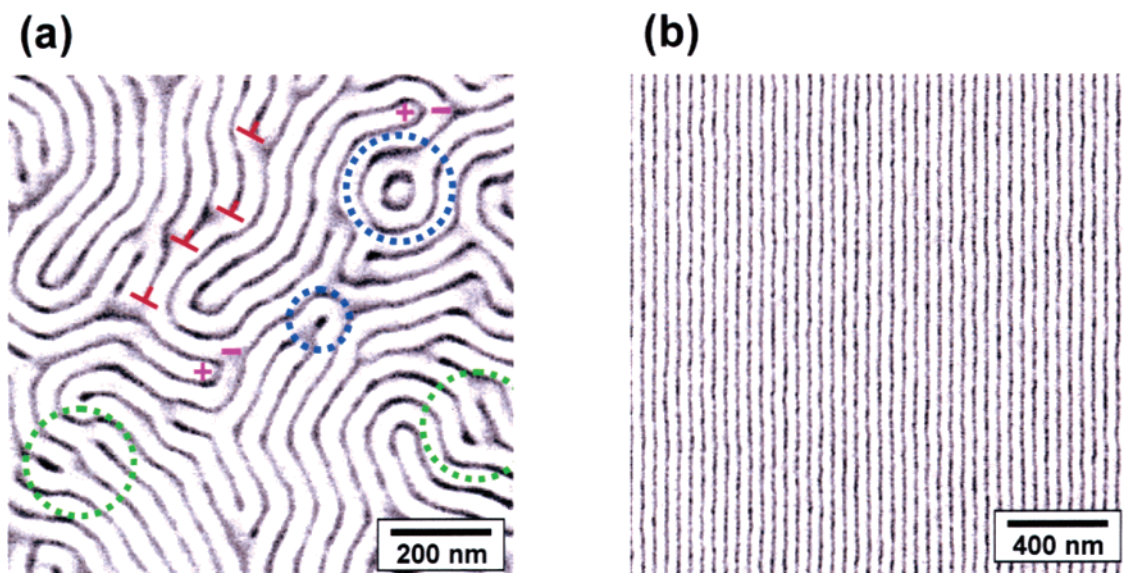
CDV

Figure 1. Top-down SEM images of a PS-*b*-PMMA copolymer (Lo = 48 nm) self-assembled on (a) a neutral homogeneous SAM surface and (b) a chemically patterned SAM surface (Ls = 47.5 nm).

It was measured in a region where several parallel lamellae were locally straight. The obtained average value was Lo = 48 nm. Phenethyltrichlorosilane (PETS) was purchased from Gelest, Inc., and deposited on the native oxide layer of a silicon wafer to prepare a chemically neutral homogeneous SAM surface. The detailed experimental procedure for SAM patterning has been presented elsewhere.[18] In brief, a thin layer (50−80 nm) of photoresist (PMMA) was spin-coated on the PETS deposited wafer and patterned by EUV interferometric lithography.[20] The topographic pattern in the photoresist was replicated into a chemical pattern in the SAM layer by high-flux X-ray radiation under an oxygen atmosphere. The SAM not protected by the photoresist layer was selectively oxidized to form a polar SAM, whereas the protected SAM was not oxidized due to oxygen blocking by the photoresist layer. An alternating neutral and polar SAM pattern that exactly replicated the topographic pattern in the photoresist layer was fabricated after removal of the photoresist by solvent washing.

Block copolymer thin films with a thickness of 60 nm were spin-coated on the homogeneous or patterned SAM surfaces and annealed at a high temperature for a sufficiently long time. The final self-assembled nanostructures of block copolymer in thin films were characterized by SEM observation. No sample treatment was applied prior to SEM characterization. Note that in the SEM images of the symmetric lamellae the darker PMMA domains appear narrower than the bright PS domains. The image contrast of PS-*b*-PMMA block copolymer without any sample treatment arises from the selective electron beam damage of the PMMA components during SEM observation. The darker domains correspond to valleys, where the PMMA was partially removed. The observed contrast primarily resulted from the topographic variation of the film thickness rather than chemical contrast.

Results and Discussion

PETS SAM deposited on a silicon wafer provided a surface with an equivalent surface tension for PS and PMMA. On the chemically neutral surface block copolymer chains oriented parallel to the surface due to the confinement imposed by the hard substrate surface, and therefore the lamellae oriented perpendicular to the substrate surface. Figure 1a shows a typical SEM image of a block copolymer thin film with a thickness of 60 nm. The top-down view of the thin film revealed the spontaneously formed layered structure. It lacked any long-range order and consisted of various combinations of defects such as edge dislocations and disclinations. Screw dislocations that are known to have the lowest free energy penalty in a bulk sample

did not appear because the distortion of the director was allowed only within the two-dimensional plane of the thin film.

The majority of defects consisted of edge dislocations. Their self-energy was lower than that of disclinations due to a weaker distortion of the director field. Either a PS or PMMA component constituted the core of the dislocation, but as shown in Figure 1a, the population of dislocations having a PMMA core was remarkably high (about 70%, PMMA core dislocations of 525 out of 827). Similar behavior has been observed for the dislocations formed in block copolymer thin films having a surface parallel orientation of lamellae.[21,22] The inclusion of a small amount of homopolymer in a sample is able to cause the spontaneous curvature of the lamellae.

Defects in the self-assembled structure of the block copolymer are able to be annihilated spontaneously upon a prolonged annealing at a high temperature.[23−25] In particular, two oppositely signed dislocations are attracted to each other and can merge to form a defect-free morphology. Pairs of oppositely signed edge dislocations that had an attractive interaction are marked by green circles in Figure 1a. The interaction between dislocations depends on their sign and positional arrangement. The repulsive interaction between the same signed dislocations was lowest when the dislocations were aligned in a row to constitute a domain wall or a tilt boundary (red symbols).[26]

As expected, most of the observed disclinations had the weakest strength of ±1/2. However, a nonnegligible number of +1 disclinations also were present (blue circle). The self-energy of an isolated disclination is large; therefore, many disclinations pair with oppositely signed disclinations in order to release the total distortion energy. Such combinations led to edge dislocations with large Burgers vectors (violet "+" and "−" marks).

The overall density of defects in thin films appeared much higher than that in bulk samples. The high interfacial area-to-volume ratio of thin film geometries could promote the density of defects. The activation energy for the nucleation of an ordered domain is usually low at interfaces where the energetic cost for the formation of a new surface is low. Thin films have a much larger interfacial area than bulk samples, resulting in a higher nucleation density and therefore a higher defect density in the self-assembled nanostructures. The limited degree of freedom for the structure evolution in the two-dimensional geometry
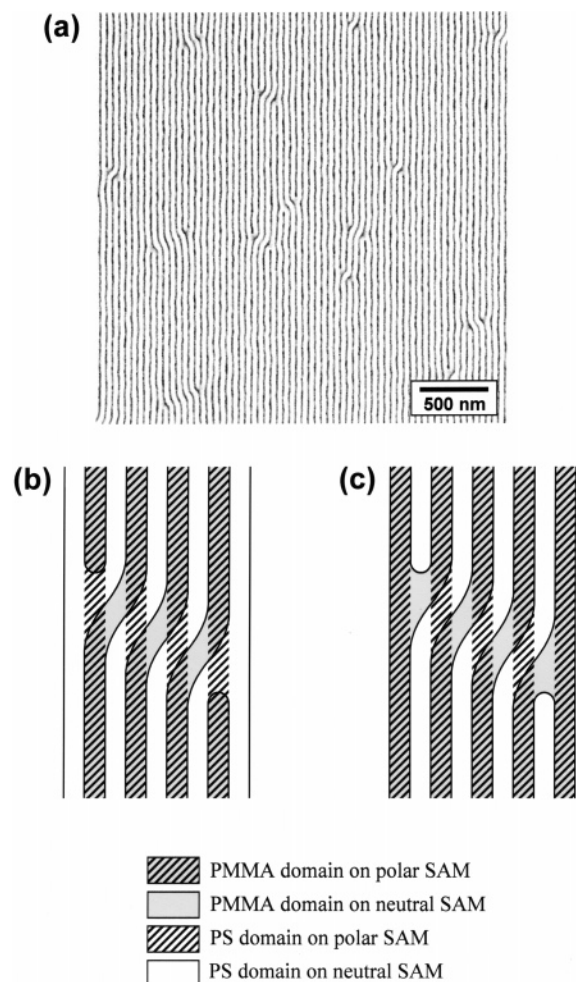
CDV

Figure 2. (a) Top-down SEM image of PS-*b*-PMMA copolymer self-assembled on a patterned surface (Ls = 45 nm). Schematic illustration of dislocation dipoles formed on a chemically patterned surface with the core components of (b) PS and (c) PMMA.

could also influence the density of defects. The movement of defects is restricted within the two-dimensional plane of the film. In this geometry the number of pathways for merging defects is limited and results in a low annihilation rate of defects.

The self-assembled nanostructures in block copolymer thin films were able to be perfectly oriented and epitaxially registered on chemically patterned surfaces by a technique known as epitaxial self-assembly.[18] When the pattern period of the surface pattern was commensurate to the lamellar period of the block copolymer, the lamellae formed well-registered defect-free structures over an arbitrarily large area. Figure 1b shows a SEM image of the registered block copolymer morphology. The surface pattern period (Ls) was 47.5 nm, which was commensurate to the natural lamellar period of the block copolymer (Lo) of 48 nm. In the present work, the chemical nature of the surface pattern consisted of alternating neutral and polar SAM, where the neutral SAM had an equivalent interfacial energy toward the PS and PMMA components but the polar SAM had a lower interfacial energy toward the PMMA than the PS. Consequently, the driving force for registration was the preferential wetting of the polar SAM by the PMMA component.

In contrast to the defect-free lamellar structures formed on a pattern with commensurate periodicity, various types of defects appeared when the surface pattern period was incommensurate with the natural block copolymer lamellar period. Figure 2a shows a representative SEM image of the block copolymer

morphology on a patterned surface having a pattern period of 45 nm. The dominant defect structure consists of a pair of oppositely directed edge dislocations. The striped surface pattern imposed an asymmetric structure (flattened toward one side) upon each dislocation. The lamellar compression enforced by the narrow surface pattern was relieved by the local bending of layers. The bent layers were enclosed by two oppositely signed edge dislocations, minimizing the distortion of the director field outside of the dipole structure. The magnitude of the Burgers vector of the dislocations corresponded to one lamellar period and maintained the weakest distortion of the director field in the block copolymer film.

The dislocations that form dipoles predominantly have PMMA cores. However, the dislocations with PMMA cores demand a larger interfacial energy than those with PS cores owing to the greater interfacial area of unfavorable contact at the film−substrate interface. Figure 2b,c schematically compares the two cases. The polar stripe prefers the PMMA domain to the PS domain, while the neutral stripe does not have any preference. If a dislocation has a PS core, the unfavorable contact is limited to the region that the bent PS lamellae between two cores meet a polar SAM surface (Figure 2b). In contrast, if a dislocation has a PMMA core, the PS domain around the core also interacts with the polar SAM surface (Figure 2c). Despite the higher interfacial energy, nearly all of the observed dislocations had a PMMA component at their cores.

A new morphology appeared when the surface pattern period was greater than the lamellar period. For surface pattern periods between 50 and 53.75 nm, the lamellae were undulated (herringbone structure) in the film plane and simultaneously tilted in the out-of-plane direction. At the pattern period of 55 nm, in addition to the herringbone and tilted structures, the lamellae that ignored the underlying surface pattern began to appear and formed a randomly oriented lamellar morphology. Further increases in the surface pattern period beyond 55 nm are expected to lead to totally disordered lamellar structures.

Parts a and b of Figure 3 are the scanning electron micrographs of in-plane and cross-sectional structures observed for the samples with Ls = 52.5 and 53.75 nm, respectively. The undulation of the lamellae is clearly presented in the in-plane view. A small number of edge dislocations were observed as a dominant defect. The edge dislocations were nucleated primarily where the oppositely directed convex layers were confronting each other (red marks in Figure 3a). In the cross-sectional view lamellae were tilted away from the film−substrate interface, and imperfect lamellae were observed at the bottom of the film where oppositely directed undulations met (red circle in Figure 3b). Note that when the differences in the periodicities of the surface pattern and lamellae were smaller (Ls = 50 nm), undulated lamellae without any defects were observed.[18]

The undulated structure has been frequently observed when various layered soft materials such as smectic liquid crystals,[27,28] lamellar block copolymers,[29−31] and amphiphilic lamellar materials[32] were mechanically dilated. When a thin film of a layered material is expanded in the layer normal direction, the undulation of the layer occurs such that the energy penalty for layer expansion is exchanged with that for layer bending. Although the final morphologies share common features, the undulated structures observed in the present research were hardly induced by mechanical dilation. Undulations from mechanical dilation would penetrate throughout the film thickness and consequently would be accompanied by the unfavorable contact of PS domains to the polar, oxidized SAM surface. A more realistic model describing the full three-dimensional structures
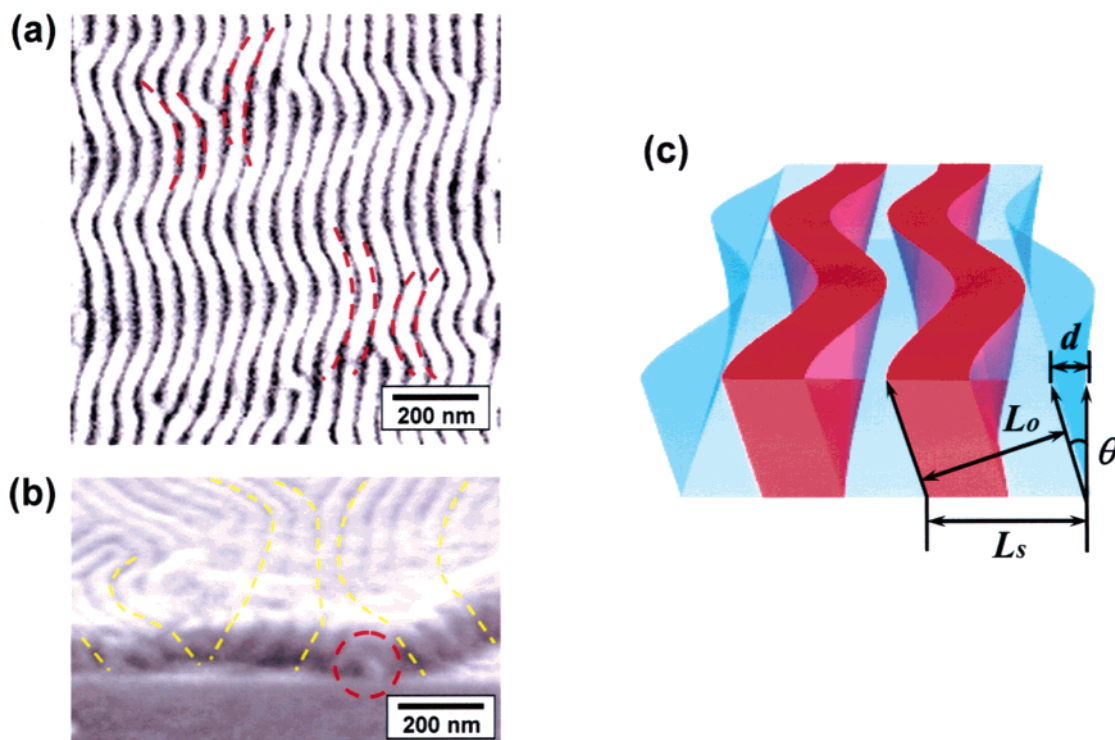
CDV

Figure 3. (a) Top-down and (b) cross-sectional SEM images of PS-*b*-PMMA copolymer thin films self-assembled on the chemically patterned surfaces with the pattern periods of 52.5 and 53.75 nm, respectively. (c) Schematic illustration of the undulated and tilted lamellar morphology. In the schematic the lamellae are tilted away from the surface normal direction in order to match with the wide surface pattern at the film−substrate interface. The maximum tilt angle, θ, is given by a simple relationship of $\cos \theta = Lo/Ls$. The undulated morphology results from tilting at the free boundary on the top surface of the film.

of the undulated lamellae observed in the present research is schematically illustrated in Figure 3c. The lamellae at the film−substrate interface are registered perfectly following the straight surface pattern. However, they are tilted away from the surface normal direction, and the undulated morphology results at the free boundary on the top side of the film. Here the maximum tilt angle, θ, is given following a simple relationship of $\cos \theta = Lo/Ls$.[33] The resulting θ values are 16° and 24° for Ls = 50 and 52.5 nm, respectively. From a film 60 nm in thickness, the maximum displacement, d, is estimated to be 17 nm for Ls = 50 nm and 27 nm for 52.5 nm. The calculated values are consistent with the experimental SEM observations. Additionally, the relationship between the curvature of the lamellae and the direction of tilting provided strong evidence supporting the model. As indicated by the yellow dotted lines in Figure 3b, the lamellae tilted toward the convexity of the undulated structure, which is consistent with the schematic drawing in Figure 3c. On the whole, the presented model successfully describes the three-dimensional structure of the tilted and undulated lamellae and does not require any unfavorable contact between the PS domains and the oxidized SAM surface. Note that in a prior research by Edwards et al.[34] lamellar expansion rather than lamellar undulation was observed for block copolymer thin films self-assembled on surface patterns with periods larger than the block copolymer lamellar period. The difference between the block copolymer morphologies presented here and the structures observed in the literature is attributed to the differences in the film thicknesses. The thickness of 40 nm used by Edwards et al.[34] was less than the one lamellar period, while the film thickness examined here was 1.25Lo. Molecular level simulations by Wang et al.[35] found that the film thickness influences the structural evolution in block copolymer thin films and that lamellae form tilted structures when the film is sufficiently thick. When the film is very thin, layer expansion

does not require a large energy penalty. As the film gets thicker, however, the energy penalty increases such that tilted morphologies become favored.

Conclusion

The defect morphologies in the lamellar block copolymer thin films on chemically neutral and patterned surfaces were investigated. Up to now the researches on the defect structure in block copolymer thin film self-assembled on nanopatterned surface have been limited to theoretical approach or simulation.[35−38] The present work provides valuable experimental results with detailed analysis. Block copolymer thin films on the homogeneous neutral surfaces formed surface perpendicular oriented lamellae. The in-plane morphology showed a disordered arrangement of lamellae with a high density of defects. Predominantly low-energy defects such as edge dislocations and ±1/2 disclinations appeared as well as a small number of +1 disclinations. The interaction between the defects induced the formation of structures such as tilt boundaries or edge dislocations with large Burgers vectors. On the chemically patterned surfaces consisting of alternating neutral and polar SAM surfaces, the lamellar block copolymer formed well-aligned, defect-free structures provided that the surface pattern period was commensurate to the natural lamellar period of the block copolymer. Lamellae were perfectly registered due to the preferential wetting of the polar SAM with the PMMA block. In contrasts, defect structures were produced when the surface pattern and lamellar periodicities were incommensurate. When the surface pattern was slightly narrower than the lamellar period, a defect structure of dislocation dipoles appeared. If the surface pattern period was slightly larger than the lamellar period, the lamellae were tilted away from the surface normal direction. The resulting morphology at the top surface of the film showed the undulated lamellae. The present work demon-

CDV

strates that the final morphologies in block copolymer thin films are influenced by dimensional parameters such as the commensurability between the periodicities of the surface pattern and the self-assembled structure and the thickness of the block copolymer film. Note that the mismatch in the periodicities as small as 4% resulted in those defect structures. It contrasts to the broad adaptabilities of sphere or surface parallel cylinder morphologies to topographic constraints[39,40] and those of surface perpendicular lamellae to chemical patterns with preferential and preferential wetting.[34] However, the aspect ratio of self-assembled structure has been limited in those approaches. To prepare defect-free nanostructures with a high aspect ratio, the surface patterns with a commensurability of the periodicities and a high chemical contrast would be required.

References and Notes

(1) Chan, V. Z.-H.; Hoffman, J.; Lee, V. Y.; Iatrou, H.; Avgeropoulos, A.; Hadjichristidis, N.; Miller, R. D.; Thomas, E. L. *Science* **1999**, *286*, 1716−1719.
(2) Park, M.; Harrison, C.; Chaikin, P. M.; Register, R. A.; Adamson, D. H. *Science* **1997**, *276*, 1401−1404.
(3) Cheng, J. Y.; Ross, C. A.; Chan, Z.-H. V.; Thomas, E. L.; Lammertink, R. G. H.; Vansco, G. *J. Adv. Mater.* **2001**, *13*, 1174−1178.
(4) Thurn-Albrecht, T.; Schotter, J.; Kästle, G.. A.; Emley, N.; Shibauchi, T.; Krusin-Elbaum, L.; Guarini, K.; Black, C. T.; Tuominen, M. T.; Russell, T. P. *Science* **2000**, *290*, 2126−2129.
(5) Lopes, W. A.; Jaeger, H. M. *Nature (London)* **2001**, *414*, 735−738.
(6) Black, C. T.; Guarini, K. W.; Milkove, K. R.; Baker, S. M.; Russell, T. P.; Tuominen, M. T. *Appl. Phys. Lett.* **2001**, *79*, 409−411.
(7) Segalman, R. A.; Yokoyama, H.; Kramer, E. J. *Adv. Mater.* **2001**, *13*, 1152−1155.
(8) Sundrani, D.; Darling, S. B.; Sibener, S. J. *Nano Lett.* **2004**, *4*, 273−276.
(9) Mansky, P.; Liu, Y.; Huang, E.; Russell, T. P.; Hawker, C. *Science* **1997**, *275*, 1458−1560.
(10) Ryu, D. Y.; Shin, K.; Drockenmuller, E.; Hawker, C. J.; Russell, T. P. *Science* **2005**, *308*, 236−239.
(11) Amundson, K.; Helfand, E.; Davis, D. D.; Quan, X.; Patel, S. S.; Smith, S. D. *Macromolecules* **1991**, *24*, 6546−6548.
(12) Morkved, T. L.; Lu, M.; Urbas, A. M.; Ehrichs, E. E.; Jaeger, H. M.; Mansky, P.; Russell, T. P. *Science* **1996**, 273−931.
(13) Angelescu, D. E.; Waller, J. H.; Adamson, D. H.; Deshpande, P.; Chou, S. Y.; Register, R. A.; Chaikin, P. M. *Adv. Mater.* **2004**, *16*, 1736−1740.
(14) Bodycomb, J.; Funaki, Y.; Kimishima, K.; Hashimoto, T. *Macromolecules* **1999**, *32*, 2075−2077.
(15) Rosa, C. D.; Park, C.; Thomas, E. L.; Lotz, B. *Nature (London)* **2000**, *405*, 433−437.
(16) Ludwigs, S.; Böker, A.; Voronov, A.; Rehse, N.; Magerle, R.; Krausch, G. *Nat. Mater.* **2003**, *2*, 744−747.
(17) Kim, S. H.; Misner, M. J.; Xu, T.; Kimura, M.; Russell, T. P. *Adv. Mater.* **2004**, *16*, 226−231.
(18) Kim, S. O.; Solak, H. H.; Stoykovich, M. P.; Ferrier, N. J.; de Pablo, J. J.; Nealey, P. F. *Nature (London)* **2003**, *424*, 411−414.
(19) Stoykovich, M. P.; Müller, M.; Kim, S. O.; Solak, H. H.; Edwards, E. W.; de Pablo, J. J.; Nealey, P. F. *Science* **2005**, *308*, 1442−1446.
(20) Solak, H. H.; David, C.; Gobrecht, J.; Golovkina, V.; Cerrina, F.; Kim, S. O.; Nealey, P. F. *Microelectron. Eng.* **2003**, *67−68*, 56−62.
(21) Liu, Y.; Rafailovich, M. H.; Sokolov, J.; Schwarz, S. A.; Bahal, S. *Macromolecules* **1996**, *29*, 899−906.
(22) Huang, E.; Mansky, P.; Russell, T. P.; Harrison, C.; Chaikin, P. M.; Register, R. A.; Hawker, C. J.; Mays, J. *Macromolecules* **2000**, *33*, 80−88.
(23) Harrison, C.; Adamson, D. H.; Cheng, Z.; Sebastian, J. M.; Sethuraman, S.; Huse, D. A.; Register, R. A.; Chaikin, P. M. *Science* **2000**, *290*, 1558−1560.
(24) Harrison, C.; Cheng. Z.; Sethuraman, S.; Huse, D. A.; Chaikin, P. M.; Vega, D. A.; Sebastian, J. M.; Register, R. A.; Adamson, D. H. *Phys. Rev. E* **2002**, *66*, 011706.
(25) Hahm, J.; Lopes, W. A.; Jaeger, H. M.; Sibener, S. J. *J. Chem. Phys.* **1998**, *109*, 10111−10114.
(26) Chandrasekhar, S. *Liquid Crystals*, 2nd ed.; Cambridge University Press: New York, 1992.
(27) Clark, N. A.; Meyer, R. B. *Appl. Phys. Lett.* **1973**, *22*, 493−494.
(28) Rosenblatt, Ch. S.; Pindak, R.; Clark, N. A.; Meyer, R. B. *J. Phys. (Paris)* **1977**, *38*, 1105−1115.
(29) Amundson, K.; Helfand, E. *Macromolecules* **1993**, *26*, 1324−1332.
(30) Wang, Z.-G. *J. Chem. Phys.* **1994**, *100*, 2298−2309.
(31) Cohen, Y.; Brinkmann, M.; Thomas, E. L. *J. Chem. Phys.* **2001**, *114*, 984−992.
(32) Guo, H.; Kremer, K. *J. Chem. Phys.* **2003**, *118*, 7714−7723.
(33) Petera, D.; Muthukumar, M. *J. Chem. Phys.* **1998**, *109*, 5101−5107.
(34) Edwards, E. W.; Montague, M. F.; Solak, H. H.; Hawker, C. J.; Nealey, P. F. *Adv. Mater.* **2004**, *16*, 1315−1319.
(35) Wang, Q. *Macromol. Theor. Simul.* **2005**, *14*, 96−108.
(36) Wang, Q.; Yan, Q.; Nealey, P. F.; de Pablo, J. J. *Macromolecules* **2000**, *33*, 4512−4525.
(37) Wang, Q.; Nath, S. K.; Graham, M. D.; Nealey, P. F. *J. Chem. Phys.* **2000**, *112*, 9996−10010.
(38) Petera, D.; Muthukumar, M. *J. Chem. Phys.* **1998**, *109*, 5101−5107.
(39) Sundrani, D.; Darling, S. B.; Sibener, S. J. *Langmuir* **2004**, *20*, 5091−5099.
(40) Cheng, J. Y.; Mayes, A. M.; Ross, C. A. *Nat. Mater.* **2004**, 823−828.

MA060087U